



1 **Investigating the effects of herbaceous root types on the soil**
2 **detachment process at the species level**

3 Jian-Fang Wang^a, Bing Wang^{a, b}, Yan-Fen Yang^{a, b*}, Guo-Bin Liu ^{a, b},
4 Feng-Bao Zhang ^{a, b}, Nu-Fang Fang ^{a, b}

5 a State Key Laboratory of Soil Erosion and Dryland Farming on the Loess Plateau, Institute of Soil
6 and Water Conservation, Northwest A&F University, Yangling, Shaanxi, 712100, PR China

7 b University of Chinese Academy of Sciences, Beijing, 100049, China

8

9 **HIGHLIGHTS**

10 The effects of plant roots on soil detachment were detected at the species level.

11 The efficiency of a fibrous root system in reducing soil detachment is 25% higher than
12 that of a tap root system.

13 Root length density can effectively reflect the effects of root type on soil detachment.

14

*Corresponding author at: State Key Laboratory of Soil Erosion and Dryland Farming on the Loess Plateau, Institute of Soil and Water Conservation, Northwest A&F University, Yangling, Shaanxi 712100, PR China.
E-mail addresses: w18691866409@163.com, yfyang@ms.iswc.ac.cn (Y.-F. Yang).
First author: (Jian-Fang Wang)



15 Abstract

16 The changes in soil properties and root traits caused by plant growth might have great effects
17 on the process of soil detachment by overland flow. On this basis, two typical herbaceous plants,
18 *Bothriochloa ischcemum* (Linn.) Keng (BI; fibrous root system) and *Artemisia vestita* Wall. ex Bess
19 (AG; tap root system), from the Loess Plateau were studied for one year under six planted densities
20 of 5 plants m⁻², 10 plants m⁻², 15 plants m⁻², 20 plants m⁻², 25 plants m⁻², and 30 plants m⁻² to
21 determine how the soil detachment rate responds to soil properties and plant root traits. In total, 24
22 steel tanks were planted, and two plots were used as bare soil controls. Their soil detachment rates
23 were tested under a constant overland flow (1.5 l s⁻¹) on a 26.2% slope. The results showed that the
24 soil detachment rate under the six planted densities ranged from 0.034 kg m² s⁻¹ to 0.112 kg m² s⁻¹
25 for BI and was ranged from 0.053 m² s⁻¹ to 0.132 m² s⁻¹ for AG, which all greatly reduced soil
26 detachment rate and were 68.17% to 92.33% and 69.20% to 87.27% less than that of the control. In
27 general, BI was more effective in reducing the soil detachment rate than AG, achieving a mean soil
28 detachment rate that was 23.75% lower. With increasing plant density, the soil detachment rate
29 decreased as a power function ($R^2 = 0.23, p < 0.01$). The overland flow hydraulic characteristics,
30 soil properties and root traits influenced by plant density were positively or negatively correlated
31 with the soil detachment rate. Specifically, the soil detachment rate decreased with velocity, bulk
32 density, root length density, and increased with shear stress and the Darcy–Weisbach friction factor
33 as power or exponential functions (R^2 ranged from 0.16 to 0.54, $p < 0.01$). On this basis, the soil
34 detachment rate (D_r) can be satisfactorily estimated by the overland flow velocity (v), soil bulk
35 density (BD) and root length density (RLD) as a power function ($D_r = 5.636v^{0.118} \times BD^{-19.917} \times$
36 $RLD^{-0.170}; R^2 = 0.58; NSE = 0.78; p < 0.01$).

37 **Key words:** soil detachment rate, root length density, overland flow, tap root system, fibrous root
38 system, Loess Plateau



39 **1 Introduction**

40 Soil erosion is a serious threat to land productivity and sustainability in both
41 natural and human-managed ecosystems (Su et al., 2014; Fu et al., 2000; Li et al., 2015).
42 Traditionally, soil erosion is affected by hydrology, soil, and vegetation (Foster, 1982),
43 for which conservation tillage, vegetation and engineering measures are used to control
44 soil loss (Rickson, 2014; García-Ruiz et al., 2015). The process of soil erosion as a
45 result of rainfall or overland flow includes soil detachment (Wang and Zhang, 2017),
46 sediment transport, and deposition (Ellison, 1947; Wu et al., 2018). Nearing et al. (1999)
47 defined soil erosion as the dislodging of soil materials from their current place at a given
48 time and area. soil detachment rate is a key parameter for both conceptually and
49 physically based soil erosion models, as changes in soil detachment rate and sediment
50 load determine whether the soil detaches or deposits (Nearing et al., 1989). For instance,
51 in the conceptually based Areal Nonpoint Source Watershed Environment Response
52 Simulation model (Beasley et al., 1980), and in the physically based models of Water
53 Erosion Prediction Project model (Nearing et al., 1999) and European Soil Erosion
54 Model (Morgan et al., 1998). In these soil erosion and sediment transport models, the
55 hydrological part of the runoff process is simulated, which is the prerequisite or driving
56 force for the occurrence of soil detachment.

57 The hydraulic characteristics of overland flow, which is affected by the
58 hydrological elements of precipitation, vegetation water holding, soil infiltration, and
59 evaporation, have a significant effect on soil detachment (Jonge L, et al., 2017). In
60 general, the soil detachment rate increases with flow discharge, runoff depth, or flow
61 velocity as a linear or power function (Zhang et al., 2002). In addition, the hydraulic
62 parameters of shear stress, stream power, and unit stream power are normally used to
63 simulate soil detachment processes. With increasing shear stress, stream power, and
64 unit stream power, the soil detachment rate decreases (Nearing et al., 1991; Hairsine
65 and Rose, 1992a, b; Zhang et al., 2002; Morgan et al., 2002). The effects of runoff
66 hydraulics characteristics on soil erosion are generally detected under given conditions.



67 In fact, runoff hydraulic parameters vary in the process of soil scouring by overland
68 flow, and these variations might be more closely related to soil detachment during soil
69 erosion. However, existing studies have not sufficiently determined these relationships.
70 Soil property is an inherent characteristic of soil mass and determines the ability of soil
71 to resist overland flow detaching. The soil texture or type of soil particle distribution,
72 soil physical property of bulk density, cohesion, aggregate stability, soil hydrological
73 properties of infiltration capacity, and soil organic matter all affect the soil detachment
74 process (Su et al., 2014; Knapen et al., 2007; Ye et al., 2017). In addition, soil moisture
75 is critical for estimating the infiltration rate and quantity of runoff generated during
76 rainfall, which greatly affects the soil detachment process (Lee and Kim; 2021). Overall,
77 with increasing clay content, bulk density, cohesion, water stable aggregates, aggregate
78 median diameter, and organic matter content (Wang et al., 2018a; Vannoppen et al.,
79 2017), and decreasing silt content and soil moisture, the soil detachment rate decreases
80 (Knapen et al., 2007; Nachtergaele and Poesen, 2002).

81 Vegetation can effectively reduce soil erosion and is often used as a biological
82 measure to control soil and water loss (Labriere et al., 2015; Liu et al., 2020; Burylo et
83 al., 2014). The reduction in soil detachment as a result of vegetation is at least half
84 attributed to the plant root system (Wang et al. 2014). The primary mechanism for plant
85 roots to reduce soil detachment is the root system binding to the soil mass and thereby
86 reinforcing the soil mass, which is called a root binding effect (De Baets et al., 2006;
87 Knapen et al., 2007; Herbrich et al., 2018). In general, soil has high compression
88 strength and low tensile strength, whereas plant roots exhibit the opposite properties
89 (Simon and Collison., 2001). Thus, when a root interweaves into a soil mass during
90 plant growth, the soil-root matrix has both high compression strength and tensile
91 strength, intensifying the soil's resistance to flowing water (Xin et al., 2016). Roots also
92 exudate secretions to stick to soil mass, which contributes to root bonding effects (Godo
93 et al., 1980). The effects of plant roots on soil erosion are also varied due to the root
94 types. For example, plants with fibrous root systems generally have many fine roots on
95 the topsoil, giving them an erosion-reducing potential that is much more significant



96 than that of tap root systems, which have large roots and fewer fine roots (Mamo and
97 Bubenzer, 2001a, b). Wang and Zhang (2017) found that the soil detachment rate in
98 grasslands with mainly tap root systems was as much as 14.7 times higher than that of
99 grasslands with mainly fibrous root systems.

100 The effects of root type differences on reducing soil detachment are reflected by
101 the root traits of biomass and root morphology, including root mass density, root
102 diameter, root length density, root surface area density, and root volume density.
103 Previous studies have mostly used root mass density to quantify the effect of roots on
104 soil detachment as it is easy to test. These studies show that the soil detachment rate
105 decreases exponentially with increasing root mass density (Gyssels and Poesen, 2003).
106 Root biomass is often highly correlated with morphological traits, enabling it to
107 represent, to a large extent, certain morphological traits. These indexes have a good
108 quantitative relationship with soil erosion. However, root biomass does not reflect soil
109 erosion caused by root morphology well when the plant species vary and their root
110 morphological traits of length, thickness, number, surface area, and volume are
111 significantly different, especially at the species level. Therefore, root morphological
112 traits should also be considered when simulating soil erosion, as they better indicate
113 how plant roots affect the process of soil erosion. Previous studies have shown that the
114 soil detachment rate decreases exponentially with root length density, root surface area
115 density, and root volume density (De Baets et al. 2006; Zhou and Shang Guan. 2005;
116 Ye et al. 2017). Plant roots also extrude soil masses and increase soil porosity during
117 growth, and these effects are more apparent when the root diameter increases (Simon
118 and Collison, 2001). Nevertheless, no significant relationship has been found between
119 root diameter and the soil erosion rate (Vannoppen et al., 2015). According to the
120 effective root density, which is a different expression of root diameter that refers to the
121 number of roots with a diameter less than 1 mm in a certain soil cross-section, a negative
122 correlation was found between root diameter and soil erosion rate (Li et al., 1991). In
123 addition, plant root morphological traits are used in hydraulic root architecture models
124 for plants that uptake water from the soil, indirectly influencing the soil erosion process



125 (Gayler et al., 2013). Whether the root system directly affects soil erosion or indirectly
126 affects soil erosion. Their effects of root morphological traits on soil erosion are obvious.

127 Previous studies have examined the efficacy of plant root systems in reducing soil
128 erosion and quantified the relationship between root traits and soil erosion rate based
129 on root type and distribution (including the indirect effects on soil erosion via changing
130 soil properties). However, most of these studies are still staying at vegetation
131 community of different land use type. Thus, the effects of different species on reducing
132 soil erosion remain unclear. To date, some hydraulic root architecture models have
133 considered root water uptake and soil water distribution at the species level, which also
134 affect the runoff process (Quijano et al., 2015). Studying the effects of plant root system
135 on soil erosion at the species level is necessary to determine the mechanism of regional
136 vegetation measures on controlling soil erosion. Although little work has been
137 conducted to specifically study the effects of plant root systems on soil erosion at
138 species level, soil samples are usually collected from natural grasslands and inevitably
139 contain surrounding plant roots, which means the sample likely includes both plants
140 with a tap root system and those with a fibrous root system. These studies seem to return
141 to the community level of previous studies. Therefore, further studies about the
142 effectiveness of plant root system in reducing soil erosion at species level was still
143 needed, which would have great advantages for clarifying the effects of plant root
144 system on controlling soil erosion and improving the accuracy of soil erosion model.

145 The Loess Plateau is an ecological security barrier of China, and is one of the most
146 severely eroded regions in the world, with mean annual erosion rates ranging from 5000
147 $\text{Mg km}^{-2} \text{yr}^{-1}$ to 10000 $\text{Mg km}^{-2} \text{yr}^{-1}$ over the past twenty years.(Fu et al., 2000; Zheng,
148 2020). To control soil erosion, the “Grain for Green” plan was implemented in 1999
149 and vegetation began to succeed naturally. Meanwhile, grassland became the primary
150 land use type (Li et al., 2015) and has variety of vegetation community. Among the
151 species present, the zonal species is BI and the dominant species is AG. Therefore, it is
152 necessary to determine the mechanism of a varied plant root system on soil erosion
153 processes at the species level on the Loess Plateau, especially regarding the essential



154 vegetation species. This research is also important for studying the response of
155 hydrology processes to soil erosion induced by vegetation recovery. Therefore, the
156 zonal species of BI with a fibrous root system and the dominant species of AG with a
157 tap root system on the Loess Plateau were selected and planted under six densities to 1)
158 illustrate varying soil properties and root traits and the corresponding variation in
159 hydraulic characteristics of overland flow and soil detachment rates; 2) study the effects
160 of hydraulic characteristics, soil properties, and root traits on soil detachment processes;
161 and 3) estimate the soil detachment rate by developing a model based on hydraulic
162 parameters, soil properties, and plant root traits.

163 **2 Materials and methods**

164 **2.1 Experimental conditions and treatment design**

165 The experiment was conducted in the Rainfall Hall of the State Key Laboratory of
166 Soil Erosion and Dryland Agriculture on the Loess Plateau, Institute of Soil and Water
167 Conservation, Ministry of Water Resources & Chinese Academy of Sciences at
168 YangLing, Shaanxi Province. Clean water and other relevant facilities were provided
169 for the scour process. To detect the effects of plant root systems on the soil detachment
170 process, two typical herbaceous plants, BI and AG, were planted in steel tanks under
171 six different planted densities of 5 plants m⁻², 10 plants m⁻², 15 plants m⁻², 20 plants m⁻²,
172 25 plants m⁻², and 30 plants m⁻². These densities represent differences in root traits
173 and their corresponding effects on soil properties. In addition, a bare soil was selected
174 as the control, representing the response of the loessal soil to the soil detachment
175 process without the influence of herbaceous plants.

176 **2.2 Planting herbaceous plants**

177 Herbaceous plants were planted in steel tanks under six different planting
178 densities, for which each planting density was repeated twice. In total, twenty-four



179 steel tanks were used for planting. Each steel tank was 2.0 m in length, 0.5 m in width
180 and 0.5 m in depth. Before planting, the steel tanks were filled with loessal soil that
181 was collected from the top soil (0 to 40 cm) of an abandoned farmland in Ansai County
182 of the Shaanxi Province. The soil organic matter content was 3.23 g kg^{-1} , pH was 8.4,
183 and the particle size distributions of the sand, silt, and clay contents were 31.16%,
184 59.31%, and 9.53%. Before filling with soil, the slope of the steel tanks was adjusted
185 to zero, and plant roots and other debris were removed from the soil using a 2 mm
186 sieve. For the process of soil filling, 5 cm of sand was laid at the bottom of the steel
187 tanks to ensure that water could penetrate smoothly and evenly. To ensure uniformity
188 in the soil bulk density in the steel tanks, the total soil weight was calculated by the
189 fill volume and the designed bulk density (1.2 g cm^{-3}). Then, the prepared soil was
190 divided 4 times to fill the steel tanks. The thickness of the filled soil in each tank was
191 10 cm. For each layer, the soil surface was raked lightly before packing the next layer
192 to eliminate discontinuity.

193 For each steel tank, BI and AG were seeded by digging 3 mm apertures in the
194 surface soil at six plant densities. After planting, the plants were watered every two days
195 and the water amount of each tank was 16 mm. To prevent the surface from forming a
196 physical crust, water was applied using a sprayer. Watering ceased when the plants
197 appeared and were left to grow naturally. Weeds were hoed every 10 days during plant
198 growth. Both types of plants experienced an entire growth period from the beginning
199 of April to the end of September (totaling 153 days). During vegetation growth, the
200 active accumulated temperature in the study area was $2184 \text{ }^\circ\text{C}$, and the total rainfall
201 amount was 517 mm. For the bare soil control, all the measures were kept the same
202 except no vegetation was planted.

203 **2.3 Soil detachment rate measurement process**

204 Each planted steel tank was adjusted to a 26.2% slope and scoured by a constant
205 overland flow (1.5 l s^{-1}) to obtain the soil detachment rate. To study the effect of
206 different root systems on the soil detachment rate, the aboveground part of the plants



207 under six plant densities was removed, leaving only the root system for the scouring
208 test. A buffering tank with the length in 0.5 m, width in 0.2 m and height in 0.5 m was
209 fixed on top of each steel tank to dissipate the flow energy, allowing water to overflow
210 smoothly and uniformly into the steel tank. The overland flow rate and the slope
211 gradient of the planted steel tank were adjusted to the designed value before scouring.
212 A plastic film was laid on the steel tank to make sure the soil was not scoured by
213 overland flow when calibrating the flow rate, and the difference in flow rate between
214 the designed and practice values was controlled to be within 2%. During scouring,
215 clean water enters the buffering tank and then enters the test soil tank. The velocity of
216 the water flow was measured at a position of 1 m in the middle of the test steel tank
217 using a fluorescent dye technique and was modified by a reduction factor according
218 to certain flow regimes (Luk and Merz, 1992). The flow velocity and water
219 temperature were measured every 5 s. When measuring the flow velocity, runoff and
220 sediment samples were collected using a plastic bucket at sampling points below the
221 catchment area. To reduce the potential effects of soil sampling on experimental results,
222 testing was generally stopped at a certain scouring depth of 2 cm (Nearing et al., 1991;
223 Zhang et al., 2002). Based on the pretest, the experiment lasted for 75 s. After scouring,
224 the collected runoff and sediment were clarified, and the sediment was dried at
225 105 °C for 24 h and weighed to calculate the soil detachment rate (Dr ; $\text{kg m}^{-2} \text{s}^{-1}$).

$$226 \quad Dr = \frac{M}{At}, \quad [1]$$

227 where M is dry weight of the sediment (kg), A is scour area (m^2), and t is time to receive
228 sediment (s).

229 The tested mean velocity was used to compute the shear stress (τ , Pa) and Darcy–
230 Weisbach friction as follows:

$$231 \quad \tau = \rho g h s, \quad [2]$$

$$232 \quad h = \frac{Q}{VB}, \quad [3]$$

$$233 \quad f = \frac{8ghs}{v^2}, \quad [4]$$

234 where ρ is the water density (kg m^{-3}), g is the gravitational acceleration (m s^{-2}), h is



235 the overland flow depth (m), s is the tangent of the slope (m m^{-1}), Q is the flow
236 discharge ($\text{m}^3 \text{s}^{-1}$), v is the mean flow velocity (m s^{-1}), and B is the steel tank width
237 (0.5 m).

238 2.4 Soil properties and root parameter measurements

239 After scouring for five days, the soil properties were measured via “S” type
240 sampling. Specifically, the bulk density was measured using a steel ring 5 cm in height
241 and 5 cm in diameter. Soil cohesion was determined using an Eijkelkamp pocket vane
242 tester. Soil aggregation was measured via a series of sieves with bore diameters of 0.25
243 mm, 0.5 mm, 1 mm, 2 mm, and 5 mm, and the soil organic matter content was measured
244 using potassium dichromate. Each soil property measurement was repeated in triplicate
245 for each steel tank, and the soil erodibility was calculated based on the soil organic
246 matter content as:

$$247 \quad K = \left\{ 0.2 + 0.3e^{-0.0256S_1\left(1-\frac{S_2}{100}\right)} \right\} \left[\frac{S_2}{n+S_2} \right]^{0.3} \left\{ 1 - \frac{0.25C}{C+e^{(3.72-2.95C)}} \right\} \left\{ 1 - \frac{0.7S_3}{S_3+e^{(-5.51+22.95S_3)}} \right\}, \quad [5]$$

248 where S_1 is the sand content (%), S_2 is the silt content (%), n is the clay content (%), C
249 is the soil organic matter content (g kg^{-1}), and $S_3=1 - \frac{S_1}{100}$.

250 After measuring the soil properties, the plant roots in each steel tank were washed.
251 The root length (RL, cm) was measured using a steel ruler (0.1 cm) and root diameter
252 (RD, mm) was measured using electronic Vernier calipers (0.01 mm). Then, the roots
253 were dried at 65 °C for 24 h and weighed to obtain the root mass (RM, kg). The root
254 diameter mean value was weighted by root length. The root surface area (RSA, m^2) and
255 volume (RV, m^3) were also calculated according to root length and diameter. Based on
256 the steel tank volume, the soil detachment capacity (0.5 m^3), the root length density
257 (RLD, km m^{-3}), root surface area density (RSAD, $\text{m}^2 \text{m}^{-3}$), root volume density (RVR,
258 $\text{m}^3 \text{m}^{-3}$), and root mass density (RMD, kg m^{-3}) were calculated as:

$$260 \quad RLD = \frac{RL}{V}, \quad [6]$$

$$261 \quad RSAD = \frac{RSA}{V}, \quad [7]$$



262
$$RVD = \frac{RV}{V}, \quad [8]$$

263
$$RMD = \frac{RM}{V}. \quad [9]$$

264

265 **2.5 Statistical analysis**

266 Pearson's correlation analyses ($p < 0.05$) and fitted curves were used to analyze
267 and quantify relationships between the soil detachment rate and hydraulic parameters,
268 soil properties, and root traits. In addition, a regression analysis was used to establish
269 a model of soil properties, root traits, and the soil detachment rate. All analyses were
270 conducted using SPSS 22.0 and Origin 2018 software.

271 **3 Results**

272 **3.1 Variation in soil properties under two grasslands**

273 The soil properties of bulk density, cohesion, water stable aggregate, soil organic
274 matter, and soil erodibility (calculated based on the EPIC model) varied greatly between
275 the six planting densities (Table 1). In particular, no significant difference was found
276 between bulk density and plant density, maximum water stable aggregate values
277 occurred when the plant density ranged from 10 plants m^{-2} to 25 plants m^{-2} , and the soil
278 organic matter content increased with increasing plant density. The cohesion and soil
279 erodibility of the BI were high when the plant density ranged from 10 plants m^{-2} to 25
280 plants m^{-2} . Meanwhile, the cohesion of AG increased with increasing plant density, and
281 no significant relationship was observed between soil erodibility and plant density. In
282 general, BI, which has a fibrous root system, had high bulk density, cohesion, water
283 stable aggregate contents, and soil organic matter content, and low soil erodibility.
284 Specifically, these soil properties of BI were, respectively, 1.01, 1.02, 1.11, and 1.73
285 times greater and 7.69% less than those of the AG. Herbaceous plant growth increased
286 soil cohesion, water stable aggregate contents, and soil organic matter, while it



287 decreased the soil bulk density and soil erodibility. The soil bulk density was 1.23 g
288 cm^{-3} for BI and 1.22 g cm^{-3} for, which are 3.15% and 3.94%, respectively, less than that
289 of the control. The soil cohesion values of BI and AG were near 4.60 kPa, and were
290 1.07 and 1.06, respectively, times greater than that of the control. The soil organic
291 matter content was 10.69 g kg^{-1} for BI and 6.19 g kg^{-1} for AG, which are 3.44 and 1.99
292 times, respectively, greater than that of the control. Finally, soil erodibility was 0.36 for
293 BI and 0.39 for AG, which are 10% and 2.5%, respectively, less than that of the control.

294 **3.2 Differences in root traits between two herbaceous plants**

295 The ratios of the maximum to minimum for the root traits of root diameter, root
296 length density, root surface density, root volume density, and root mass density varied
297 between 4.89 and 110.58, exhibiting significant differences in these root traits under
298 six plant densities (Figure 1). With increasing plant density, changes in the root
299 diameter of the two herbaceous plants were very small and the difference between the
300 maximum and minimum was less than 0.1 mm. Other root traits, including root length
301 density, root surface area density, root volume density, and root mass density, had high
302 values when the plant density ranged from 15 plants m^{-2} to 25 plants m^{-2} . These root
303 traits also showed significant differences between BI and AG (Figure 1). Specifically,
304 BI, which has a fibrous root system, had relatively high mean root length density (19.97
305 km m^{-3}), root surface area density (9.68 $\text{m}^2 \text{m}^{-3}$), and root mass density (1.55 kg m^{-3})
306 values, which were 3.83, 1.25, and 1.31, respectively, times greater than that of AG,
307 which has a tap root system. Meanwhile, the mean root diameter and root volume
308 density values of BI were low, and were 79.56% and 82.09% less than that of AG,
309 respectively. Thus, remarkable relationships were observed among plant root traits. In
310 particular, the root length density, root mass density, and root surface area density were
311 positively correlated ($p < 0.01$; Table 2). Significant relationships among the root traits
312 and soil properties were also detected (Table 2). For example, root mass density and
313 root surface area density were positively correlated to soil cohesion ($p < 0.05$), and root



314 length density was positively correlated with soil cohesion and soil bulk density ($p <$
315 0.05).

316 **3.3 Variation in hydraulic characteristics and soil detachment rate between two** 317 **herbaceous plants**

318 The hydraulic parameters of velocity, shear stress, and Darcy–Weisbach friction
319 factor varied significantly according to plant density (Table 3). The velocity of BI was
320 the smallest when the plant density was 15 plants m^{-2} , whereas the smallest velocity for
321 AG occurred at a plant density of 5 plants m^{-2} . For both grasslands, minimum shear
322 stress and Darcy–Weisbach friction factor values occurred when the plant density
323 ranged from 15 plants m^{-2} to 25 plants m^{-2} . In general, BI had a high velocity, and low
324 shear stress and Darcy–Weisbach friction factor. The hydraulic parameters of BI ranged
325 from 1.02 to 1.56 times greater, and from 1.51% to 40.31% and 5.81% to 78.15% less
326 than that of those of AG, respectively.

327 In addition, the soil detachment rates varied significantly according to planting
328 densities for both herbaceous plants (Figure 2). Regarding BI, the soil detachment rates
329 ranged from 0.034 $kg\ m^{-2}\ s^{-1}$ to 0.112 $kg\ m^{-2}\ s^{-1}$ with a mean value of 0.061 $kg\ m^{-2}\ s^{-1}$,
330 while the soil detachment rate of AG ranged from 0.053 $kg\ m^{-2}\ s^{-1}$ to 0.132 $kg\ m^{-2}\ s^{-1}$
331 with a mean value of 0.080 $kg\ m^{-2}\ s^{-1}$. Compared with the control, the soil detachment
332 rates of these grasslands were 68.17% to 92.33% and 69.20% to 87.27% lower,
333 respectively. In general, the effects of BI on reducing the soil detachment rate was much
334 more effective than AG as its mean soil detachment rate was 23.75% lower. With
335 increasing plant density, the soil detachment rate decreased as a power function (Figure
336 3, $p < 0.01$). Regarding the hydraulic parameters of velocity, shear stress, and Darcy–
337 Weisbach friction factor, the velocity was negatively correlated with the soil
338 detachment rate, exhibiting a power function relationship. Conversely, the shear stress
339 and Darcy–Weisbach friction factor were positively correlated with soil detachment rate.
340 With increasing shear stress and Darcy–Weisbach friction factor, the soil detachment
341 rate increased as a power function (Figure 4, R^2 ranged from 0.16 to 0.26, $p < 0.01$).



342 Regarding soil properties, bulk density was negatively correlated with the soil
343 detachment rate. Specifically, with increasing bulk density, the soil detachment rate
344 increased as a power function (Figure 5, $R^2 = 0.54$, $p < 0.01$). Finally, regarding root
345 traits, root length density was negatively correlated with the soil detachment rate,
346 exhibiting an exponential function relationship (Figure 6, $R^2 = 0.24$, $p < 0.01$). On this
347 basis, the soil detachment rate (D_r) could be estimated by the velocity (v), soil bulk
348 density (BD), and root length density (RLD) as a power function ($R^2 = 0.58$, $p < 0.01$;
349 Eq. [10]).

$$350 \quad D_r = 5.636v^{0.118} \times BD^{-19.917} \times RLD^{-0.170}, \quad [10]$$

351 where the standardized coefficients of v , BD , and RLD are 0.049, -0.352, and -0.572,
352 respectively. The performance of Eq. [10] seemed satisfactory as it had a determination
353 coefficient (R^2) of 0.58 and a Nash–Sutcliffe efficiency coefficient (NSE) of 0.78
354 (Figure 7).

355 **4 Discussion**

356 **4.1 Effects of hydraulic characteristics on soil detachment**

357 Overland flow is the driving force of soil erosion and, in general, its hydraulic
358 characteristics significantly affect soil detachment. Flow velocity is commonly used to
359 reflect the speed of flowing water. A slow velocity refers to a low kinetic energy
360 overland flow, which would increase the hydraulic radius, thereby increasing shear
361 stress. Besides, the viscosity and friction increase when flow velocity slows, which
362 increases the Darcy–Weisbach friction factor. Gong (2011) found that under slow flow
363 velocity, large shear stress, and high Darcy–Weisbach friction factor conditions, soil
364 erosion is reduced. Contrary to previous studies, this study found that the soil
365 detachment rate decreased with flow velocity as a power function (Figure 4). This is
366 mainly because the influence of velocity on soil detachment is relatively weak as
367 compared with the influence of soil properties and plant root system. Thus, using the



368 flow velocity to determine the soil detachment rate may not be appropriate. As given
369 by Eq. [10], when hydraulic characteristics, soil properties, and root traits are used in
370 combination to estimate the soil detachment rate, the results show that the soil
371 detachment rate increases with flow velocity. Further, the standardized velocity
372 coefficients given in Eq. [10] were almost an order of magnitude smaller than the bulk
373 density and root length density. This confirms our theory that soil detachment is
374 primarily affected by soil properties and plant root. Both the flow shear stress and
375 Darcy–Weisbach friction factor are mainly affected by the surface resistance of
376 sediment particles and underlying surface roughness. During the process of soil erosion,
377 especially when erosion rill occurs and soil particles become eroded, soil surface
378 undulation increases, thereby increasing the overland flow form shear stress and form
379 resistance. This concept is consistent with our results, which showed that the soil
380 detachment rate increased via power functions with shear stress and Darcy–Weisbach
381 friction factor. In addition, the presence of vegetation increased form resistance, which
382 further increased the Darcy–Weisbach friction factor and the soil detachment rate.

383

384 **4.2 Effects of soil properties on soil detachment rate**

385 Differences in soil properties reflect the ability of soil mass to resist soil erosion.
386 In particular, bulk density represents the compatibility of soil mass. As bulk density
387 increases, soil mass, in general, becomes more compact and soil cohesion improves,
388 making the soil mass more resistant to detach as a result of flowing water (Chen et al.,
389 2007). Clumping fine soil particles together into firm stable aggregates, which is known
390 as soil aggregation, is a basic unit of soil structure and reflects the stability of soil. Water
391 stable aggregates are often used as indicators of soil susceptibility to flowing water
392 erosion. A high number of water stable aggregates would promote soil stability, increase
393 soil resistance to flowing water erosion, and thus reduce the soil detachment rate (Wang
394 et al., 2018b). During the formation of soil aggregates, the soil organic matter content
395 improves. Soil organic matter is commonly used to represent soil nutrients (Geng et al.
396 2015). Previous studies indicate that soil organic matter increases adhesion between
397 soil particles, making the soil mass harder to detach (Knape et al., 2007). Our results



398 were consistent with previous research, showing that the soil detachment rate is
399 negatively correlated with soil bulk density, cohesion, water stable aggregates, and soil
400 organic matter, and the soil detachment rate decreased with increasing bulk density as
401 a power function. However, the correlations between the soil detachment rate and
402 cohesion, water stable aggregates, and organic matter were not significant. This is
403 probably because the herbaceous plants were only planted for one year, and the
404 formation of soil aggregates generally requires three to five years of vegetation
405 (Semmel et al., 1990). Low soil cohesion, water stable aggregates, and organic matter
406 content lead to weak effects on soil detachment. Meanwhile, soil erodibility refers to
407 soil erosion resistance to flowing water and is calculated using the soil organic matter
408 content and soil particle composition, based on the EPIC model. A high soil erodibility
409 indicates that the soil mass is easily eroded by flowing water. In this study, soil
410 erodibility was positively correlated with the soil detachment rate. Although the
411 correlation between the soil detachment rate and soil erodibility was not significant
412 because of the low organic matter content, overall, the plant roots of the herbaceous
413 plants still reduced soil erodibility, thereby reducing soil detachment. Further,
414 differences in soil properties were also observed between BI and AG. Compared with
415 AG, BI had high bulk density, soil cohesion, water stable aggregate contents, and soil
416 organic matter, and low soil erodibility, which led to a low soil detachment rate.

417 **4.3 Effects of root system on soil detachment**

418 Plant root systems can significantly reduce the soil detachment rate. IN this study,
419 this effect varied between BI and AG because of differences in their root types. For
420 example, BI, which has a fibrous root system, a large number of roots are distributed
421 on the topsoil, making the root system more effective in preventing soil erosion. results
422 were consistent with the previous research (De Baets et al. 2006; Wang et al. 2018b),
423 revealing that the soil detachment rate of BI was 23.751% lower than that of AG, which
424 has a tap root system. Previous studies have attributed this difference in the effect of
425 plant root type on soil erosion to the root biomass (Herbrich et al., 2018). A plant root



426 system with high biomass indicates that the root system has a strong ability to reinforce
427 the soil, thereby reducing soil erosion (Wang et al., 2021). In this study, soil detachment
428 did not appear to be sensitive to root biomass and no significant relationship was found
429 between the soil detachment rate and root mass density. This indicates that root mass
430 density only reflects root biomass and might not explain the difference in root
431 morphological characteristics very well. Thus, the aforementioned difference in soil
432 detachment rate caused by the different root types in BI and AG are actually the result
433 of differences in root morphological traits, including root diameter, root length density,
434 root surface area density, and root volume density (Zhou and Shangguan. 2005).
435 Regarding root diameter, both significantly positive and negative relationships between
436 root diameter and soil detachment rate have been detected in previous studies,
437 indicating the plant root diameter is an important variable for the soil erosion process
438 (De Baets et al., 2007; Ye et al., 2017). However, some studies found no significant
439 correlation between root diameter and the soil detachment rate, indicating that their
440 relationship cannot be directly established. Rather, a relationship can only be observed
441 when the root diameter is expressed as the number of plant roots (diameter less than 1
442 mm) within a soil cross-section, which was proposed as the effective root density by Li
443 et al. (2015). In our study, no relationship was observed between the soil detachment
444 rate and root diameter. This is probably because the difference between the maximum
445 and minimum root diameters was less than 0.1 mm, and this change is too small to
446 reflect the soil detachment rate well. A long root length signifies that more plant roots
447 are interspersed in the soil mass, increasing resistance to overland flow scouring and
448 enhancing the resistance of the soil mass. Thus, the soil detachment rate decreases with
449 root length density as a power function (Figure 5). A large root surface area refers to a
450 large contact area between the plant roots and soil, and root volume represents more
451 plant roots grown in the soil, which all indicate that soil stability is strengthened,
452 making it difficult to detach the soil mass via flowing water. Although some previous
453 studies have shown that the soil erosion rate decreases with root surface area density or
454 root volume density, no significant relationships were found between the soil



455 detachment rate and root surface area density or root volume density in this study.
456 Regarding root surface area density, because of the poor correlation between root
457 diameter and soil detachment rate, the root surface area density is generally calculated
458 by both root length and root diameter, as reported by previous studies (Manoli et al.,
459 2014). For root volume density, a high value does not indicate that the effects of the
460 plant root system on reducing soil erosion are enhanced. Wang et al. (2021) found that,
461 when there is little difference in root volume, an herbaceous plant with a fibrous root
462 system generally has a long root length, which results in a strong ability to bind and
463 bond with the soil mass, making its effects on reducing soil detachment more effective
464 than that of an herbaceous plant with a fibrous root system. In other words, root volume
465 density may not be a good root parameter for reflecting the relationship between plant
466 root type and soil detachment.

467 **5 Conclusions**

468 In this study, we found that the soil detachment rate significantly decreased as a
469 power function ($R^2 = 0.23$, $p < 0.01$), with increasing plant density for two herbaceous
470 plants, becoming 85.80% and 81.19% lower than that of the control for the BI and AG
471 grasslands, respectively. The soil detachment rate also exhibited different behaviors
472 according to two plant root type. In general, BI, which has a fibrous root system,
473 effectively reduced the soil detachment rate, achieving a mean soil detachment rate that
474 was 23.75% less than that of AG, which has a tap root system. The hydraulic
475 characteristics of flow velocity, shear stress, and Darcy–Weisbach friction factor were
476 found to be correlated to the soil detachment rate ($p < 0.01$), which decreased with
477 increasing velocity and increased with shear stress and the Darcy–Weisbach friction
478 factor as power functions (mean R^2 ranged from 0.16 to 0.26, $p < 0.01$). The effects of
479 soil properties on the soil detachment rate were also varied greatly as a result of
480 differences in plant density and plant species. Specifically, the soil detachment rate
481 decreased with increasing bulk density as a power function ($R^2 = 0.54$, $p < 0.01$). The



482 different soil detachment rates caused by root types can be explained well using root
483 traits, including root length density, root surface area density, root volume density, and
484 the root biomass trait of root mass density, which all affected the soil detachment rate.
485 In particular, an exponential function was observed between root length density and the
486 soil detachment rate ($R^2 = 0.24$, $p < 0.01$). In general, the soil detachment rate could be
487 estimated effectively using the overland flow velocity, soil bulk density, and root
488 surface length density ($Dr = 5.636v^{0.118} \times BD^{-19.917} \times RLD^{-0.170}$). The
489 performance of the model developed in this study was satisfactory ($R^2=0.58$;
490 $NSE=0.78$).

491 **CRedit authorship contribution statement**

492 **Jian-Fang Wang**: Conceptualization, Methodology, Field work, Writing. **Bing Wang**:
493 Methodology, Field work, Reviewing and Editing. **Yan-Fen Yang**: Conceptualization,
494 Methodology, Reviewing and Editing, Supervision. **Guo-Bin Liu**: Reviewing and
495 Editing. **Feng-Bao Zhang**: Reviewing and Editing. **Nu-Fang Fang**: Reviewing and
496 Editing.
497 All authors have read and agreed to the published version of the manuscript.

498 **Declaration of competing interest**

499 The authors declare that they have no known competing financial interests or
500 personal relationships that could have appeared to influence the work reported in this
501 paper.

502 **Acknowledgments**

503 This work was supported by National Natural Science Foundation of China
504 (42130717), and the Chinese Academy of Sciences (CAS) "Youth Scholar of West



505 China" program (XAB2019A04). We should also thank to the Ansai Research Station
506 of Soil and Water Conservation, Chinese Academy of Sciences, Ministry of Water
507 Resource, and the State Key Laboratory of Soil Erosion and Dryland Farming on the
508 Loess Plateau, Institute of Soil and Water Conservation, Northwest A&F University for
509 technical help.

510 **References**

- 511 Beasley DB, Huggins LF, Monke EJ. ANSWERS: a model for watershed planning. *T ASABE*
512 23(4):938–0944, 1 dio:10.13031/2013.34692, 1980.
- 513 Burylo, M., Dutoit, T., Rey, F., Species traits as practical tools for ecological restoration of marly
514 eroded lands. *Restor. Ecol.* 22, 633–640, <https://doi.org/10.1002/esp.3248>, 2014.
- 515 Chen, L., W. Wei, B. Fu, and Y. Lü. Soil and water conservation on the Loess Plateau in China:
516 Review and perspective. *Prog. Phys. Geogr.* 31:389–403, [https://doi.org/10.1177/0309133307081](https://doi.org/10.1177/0309133307081290)
517 [290](https://doi.org/10.1177/0309133307081290), 2007.
- 518 De Baets, S., Poesen, J., Gyssels, G., Knapen, A., Effects of grass roots on the erodibility of top
519 soils during concentrated flow. *Geomorphology* 76, 54–67. [https://doi.org/10.1016/j.geomorph.](https://doi.org/10.1016/j.geomorph.2005.10.002)
520 [2005.10.002](https://doi.org/10.1016/j.geomorph.2005.10.002), 2006.
- 521 De Baets, S., Poesen, J., Knapen, A & Galindo, P. Impact of root architecture on the erosion–
522 reducing potential of roots during concentrated flow. *Earth Surface Processes and Landforms.* 32
523 (9), 1323–1345. <https://doi.org/10.1002/esp.1470>, 2007.
- 524 Ellison, W.D., Soil erosion studies: Part I. *Agric. Eng.* 28, 145–146, 1947.
- 525 Foster, G. Modeling the erosion process. In: C.T. Haan and D.L. Brakensiek, editors, *Hydrologic*
526 *modeling of small watersheds.* Am. Soc. Agric. Engineers, St. Joseph, MI. p. 295–380. 1982.
- 527 Fu, B., L. Chen, K. Ma, H. Zhou, and J. Wang. The relationships between land use and soil
528 conditions in the hilly area of the Loess Plateau in northern Shaanxi, China. *Catena* 39:69–78,
529 [https://doi.org/10.1016/S0341-8162\(99\)00084-3](https://doi.org/10.1016/S0341-8162(99)00084-3), 2000.
- 530 García-Ruiz, J.M., Beguería, S., Nadal-Romero, E., González-Hidalgo, J.C., Lana-Renault, N.,
531 Sanjuán, Y., A meta-analysis of soil erosion rates across the world. *Geomorphology* 239, 160–173,
532 <https://doi.org/10.1007/s11104-010-0382-6>, 2015
- 533 Gayler, S., Ingwersen, J., Priesack, E., Wohling, T., Wulfmeyer, V., and Streck, T.: Assessing the
534 relevance of subsurface processes for the simulation of evapotranspiration and soil moisture
535 dynamics with CLM3.5: comparison with field data and crop model simulations, *Environ. Earth*
536 *Sci.*, 69, 415–427, <https://doi.org/10.1007/s12665-013-2309-z>, 2013.
- 537 Geng, R., Zhang, G.H., Li, Z.W., Wang, H., Spatial variation in soil resistance to flowing water
538 erosion along a regional transect in the Loess Plateau. *Earth Surf. Process. Landf.* 40, 2049–2058,
539 <https://doi.org/10.1002/esp.3779>, 2015..
- 540 Gong J G, Jia Y W, Zhou Z H, et al. An experimental study on dynamic processes of ephemeral
541 gully erosion in loess landscapes. *Geomorphology*, 125, 203–213, [https://doi.org/10.1016/j.geomorph.](https://doi.org/10.1016/j.geomorph.2010.09.016)
542 [2010.09.016](https://doi.org/10.1016/j.geomorph.2010.09.016), 2011.



- 543 Godo G H, Reisenauer H M. Plant Effects on Soil Manganese Availability. Soil Science Society of
544 America Journal, 44, 993-995, <https://doi.org/10.2136/sssaj1980.03615995004400050024x>, 1980.
- 545 Gyssels, G., Poesen, J., The importance of plant root characteristics in controlling concentrated flow
546 erosion rates. Earth Surf. Process. Landf. 28, 371–384, <https://doi.org/10.1191/0309133305>
547 pp443ra, 2003.
- 548 Hairsine, P.B., Rose, C.W., Modeling water erosion due to overland flow using physical principles.
549 1. Sheet flow. Water Resour. Res. 28, 237–243, <https://doi.org/10.1029/91WR02380>, 1992a.
- 550 Hairsine, P.B., Rose, C.W., Modeling water erosion due to overland flow using physical principles.
551 2. Rill flow. Water Resour. Res. 28, 245–250, <https://doi.org/10.1029/91WR02381>, 1992b.
- 552 Herbrich, Marcus, Gerke, et al. Root development of winter wheat in erosion-affected soils
553 depending on the position in a hummocky ground moraine soil landscape. Journal of plant nutrition
554 and soil science, 181, 147-157, <https://doi.org/info:doi/10.1002/jpln.201600536>, 2018.
- 555 Jonge L, Moldrup P, Jacobsen O H. Soil-Water Content Dependency of Water Repellency in Soils.
556 Soil Science, 172, 577-588, <https://doi.org/10.1097/SS.0b013e318065c090>, 2017.
- 557 Knapen, A., Poesen, J., Govers, G., Gyssels, G., Nachtergaele, J., Resistance of soils to concentrated
558 flow erosion: a review. Earth. Rev. 80, 75–109, <https://doi.org/10.1016/j.earscirev.2007.08.001>,
559 2007.
- 560 Labriere, N., Locatelli, B., Laumonier, Y., Freycon, V., Bernoux, M., Soil erosion in the humid
561 tropics: a systematic quantitative review. Agric. Ecosyst. Environ. 203, 127–139,
562 <https://doi.org/10.1016/j.agee.2015.01.027>, 2015.
- 563 Lee Eunhyung and Kim Sanghyun. Characterization of soil moisture response patterns and hillslope
564 hydrological processes through a self-organizing map. Hydrol. Earth Syst. Sci., 25, 5733–5748,
565 <https://doi.org/10.5194/hess-25-5733-2021>, 2021.
- 566 Li, Y., Zhu, X.M., Tian, J.Y. Effectiveness of plant roots to increase the anti-scourability of soil on
567 the loess plateau. Chin. Sci. Bull. 36 (24), 2077–2082.1991.
- 568 Li, Z. W., G. H. Zhang, R. Geng, and H. Wang. Rill erodibility as influenced by soil and land use
569 in a small watershed of the Loess Plateau, China. Biosystems Eng. 129:248–257,
570 <https://doi.org/10.1016/j.2015>.
- 571 Liu, J. X., Liu, G. B., Dennis. C., Wang, B., Wang, Z. Y., Xiao, J., Effects of soil-incorporated plant
572 litter morphological characteristics on the soil detachment process in grassland on the Loess Plateau
573 of China. Science of the Total Environment. 705, 13465, <https://doi.org/10.1016/j.scitotenv.2020.134651>, 2020.
- 574
575 Luk, S., Merz, W. Use of the salt tracing technique to determine the velocity of overland flow. Soil
576 Technol. 5, 289-301. 1992.
- 577 Mamo, M., Bubbenzer, G., Detachment rate, soil erodibility, and soil strength as influenced by living
578 plant root part I: laboratory study. Trans. ASAE 44, 1167–1174, <https://doi.org/10.13031/2013.6445>, 2001a.
- 579
580 Mamo, M., Bubbenzer, G., Detachment rate, soil erodibility, and soil strength as influenced by living
581 plant root part II: field study. Trans. ASAE 44, 1175–1181, <https://doi.org/10.13031/2013.6446>,
582 2001b.
- 583 Manoli, Bonetti, Domec, et al. Tree root systems competing for soil moisture in a 3D soil-plant
584 model. ADV WATER RESOUR, 6, 32-42, <https://doi.org/10.1016/j.advwatres.2014.01.006>, 2014.
- 585 Morgan, R.P.C., J.N. Quinton, R.E. Smith, G. Govers, J.W.A. Poesen, K. Auerswald, et al. The
586 European Soil Erosion Model (EUROSEM): A dynamic approach for predicting sediment transport



- 587 from fields and small catchments. *Earth Surf. Processes Landforms* 23:527–544.
588 doi:10.1002/(SICI)1096-9837(199806)23:6<527::AID-ESP868>3.0.CO;2-5, 1998.
- 589 Morgan, R.P.C., Quinton, J.N., Smith, R.E., Govers, G., Poesen, J.W.A., Auerswald, Chisci,
590 Nachtergaele, J., Poesen, J., Spatial and temporal variations in resistance of loess-derived soils to
591 ephemeral gully erosion. *Eur. J. Soil Sci.* 53 (3), 449–463, [https://doi.org/10.1079/](https://doi.org/10.1079/9780851990507.019)
592 [9780851990507.019](https://doi.org/10.1079/9780851990507.019), 2002.
- 593 Nearing, M.A., G.R. Foster, L.J. Lane, and S.C. Finkner. 1989. A process-based soil-erosion model
594 for USDA-Water Erosion Prediction Project Technology. *Trans. ASAE* 32:1587–1593.
595 doi:10.13031/2013.31195, 1989.
- 596 Nearing, M. A., Bradford, J. M., Parker, S. C., Soil detachment by shallow flow at low slopes. *Soil*
597 *Sci. Soc. Am. J.* 55 (2), 339–344, <https://doi.org/10.2136/sssaj.1991.0361599500550.0020006x>,
598 1991.
- 599 Nearing, M. A., Simanton, J. R., Norton, L. D., Bulygin, S. J., Stone, J., USDA, A., Soil erosion by
600 surface water flow on a stony, semiarid hillslope. *Earth Surf. Proc. Land.* 24 (8), 677–686,
601 [https://doi.org/10.1002/\(SICI\)1096-9837\(199908\)24:83.0.CO;2-1](https://doi.org/10.1002/(SICI)1096-9837(199908)24:83.0.CO;2-1), 1999.
- 602 Quijano, J. C. and Kumar, P.: Numerical simulations of hydraulic redistribution across climates:
603 The role of the root hydraulic conductivities, *Water Resour. Res.*, 51, 8529–8550,
604 <https://doi.org/10.1002/2014wr016509>, 2015.
- 605 Rickson, R.J., Can control of soil erosion mitigate water pollution by sediments? *Sci. Total Environ.*
606 468, 1187–1197, <https://doi.org/10.1016/j.scitotenv.2014.12.086>, 2014.
- 607 Semmel H, Horn R, Hell U, Dexter A.R, Schulze E.D, The dynamics of soil aggregate formation
608 and the effect on soil physical properties, *Soil Technology*, 3, 113-129,
609 [http://doi.org/10.1016/S0933-3630\(05\)80002-9](http://doi.org/10.1016/S0933-3630(05)80002-9), 1990.
- 610 Simon, A., Collison, A., Scientific basis for streambank stabilization using riparian vegetation.
611 Proceedings of the 7th Federal Interagency Sedimentation Conference, March 25–29, Reno, Nevada,
612 V47–V54, <https://doi.org/10.1002/esp.287>, 2001.
- 613 Su, Z.L., Zhang, G.H., Yi, T., Liu, F., Soil detachment capacity by overland flow for soils of the
614 Beijing region. *Soil Res.* 179, 446–453, <https://doi.org/10.1097/SS.000000000000089>, 2014.
- 615 Vannoppen, W., De Baets, S., Keeble, J., Dong, Y., Poesen, J., How do root and soil characteristics
616 affect the erosion-reducing potential of plant species. *Ecol. Eng.* 109, 186–195,
617 <https://doi.org/10.1016/j.earscirev.2017.08.011>, 2017.
- 618 Wang, B., G.H. Zhang, X.C. Zhang, Z.W. Li, Z.L. Su, T. Yi, et al. Effects of near soil surface
619 characteristics on soil detachment by overland flow in a natural succession grassland. *Soil Sci. Soc.*
620 *Am. J.* 78:589–597. doi:10.2136/sssaj2013.09.0392, 2014.
- 621 Wang, B., Zhang, G.H. Quantifying the binding and bonding effects of plant roots on soil
622 detachment by overland flow in 10 typical grasslands on the Loess Plateau. *Soil Sci. Soc. Am. J.* 81,
623 1567–1576, <https://doi.org/10.2136/sssaj2017.07.0249>, 2017.
- 624 Wang, B., Zhang, G.H., Yang, Y.F., Li, P.P., Liu, J.X., The effects of varied soil properties induced
625 by natural grassland succession on the process of soil detachment. *Catena* 166, 192–199,
626 <https://doi.org/10.1016/j.agee.2018.07.016>, 2018a.
- 627 Wang, B., Zhang, G.H., Yang, Y.F., Li, P.P., Liu, J.X., Response of soil detachment capacity to
628 plant root and soil properties in typical grasslands on the Loess Plateau. *Agri. Ecosyst. Environ.* 266,
629 68–75, <https://doi.org/10.1016/j.agee.2018.07.016>, 2018b.



- 630 Wang, B., Li, P. P., Huang, C.H., Liu, G. B & Yang, Y. F. Effects of root morphological traits on
631 soil detachment for ten herbaceous species in the Loess Plateau. *Science of the Total Environment*,
632 754 (14),142304. <https://doi.org/10.1016/j.scitotenv.2020.142304>, 2021.
- 633 Wu, B., Wang, Z., Zhang, Q., Shen, N., Distinguishing transport-limited and detachment limited
634 processes of inter-rill erosion on steep slopes in the Chinese loessial region. *Soil Tillage Res.* 177,
635 88–96, <https://doi.org/10.1016/j.still.2018.104661>, 2018.
- 636 Xin, Z., Qin, Y., Yu, X., Spatial variability in soil organic carbon and its influencing factors in a
637 hilly watershed of the Loess Plateau, China. *Catena* 137, 660–669, [https://doi.org/10.1016/](https://doi.org/10.1016/j.catena.2016.01.028)
638 [j.catena.2016.01.028](https://doi.org/10.1016/j.catena.2016.01.028), 2016.
- 639 Ye, Z. L., Guo, Z.X. Li, C.F. Cai., The effect of baaiagrass roots on soil erosion resistance of Aquults
640 in subtropical China. *Geomorphology*,285, 82–93, [https://doi.org/10.1016/j.geomorph.](https://doi.org/10.1016/j.geomorph.2017.02.003)
641 [2017.02.003](https://doi.org/10.1016/j.geomorph.2017.02.003), 2017.
- 642 Zhang, G. H., Liu, B. Y., Nearing, M. A., Huang, C. H., Zhang, K. L., Soil detachment by shallow
643 flow. *Trans. ASAE* 45 (2), 351–357, <https://doi.org/10.13031/2013.8527>, 2002.
- 644 Zheng, H., Xiao, Y. C., Yan, H. L., et al. Quantifying the rill–detachment process along a saturated
645 soil slope. *Soil and Tillage Research*.204, 1–9, <https://doi.org/10.1016/j.still.2020.104726>, 2020.
- 646 Zhou, Z. C., and Z. P. Shang Guan. Soil anti–scourability enhanced by plant roots. *J. Integ Plant*
647 *Biol.* 47:676–682, <https://doi.org/10.1111/j.1744-7909.2005.00067.x>, 2005.

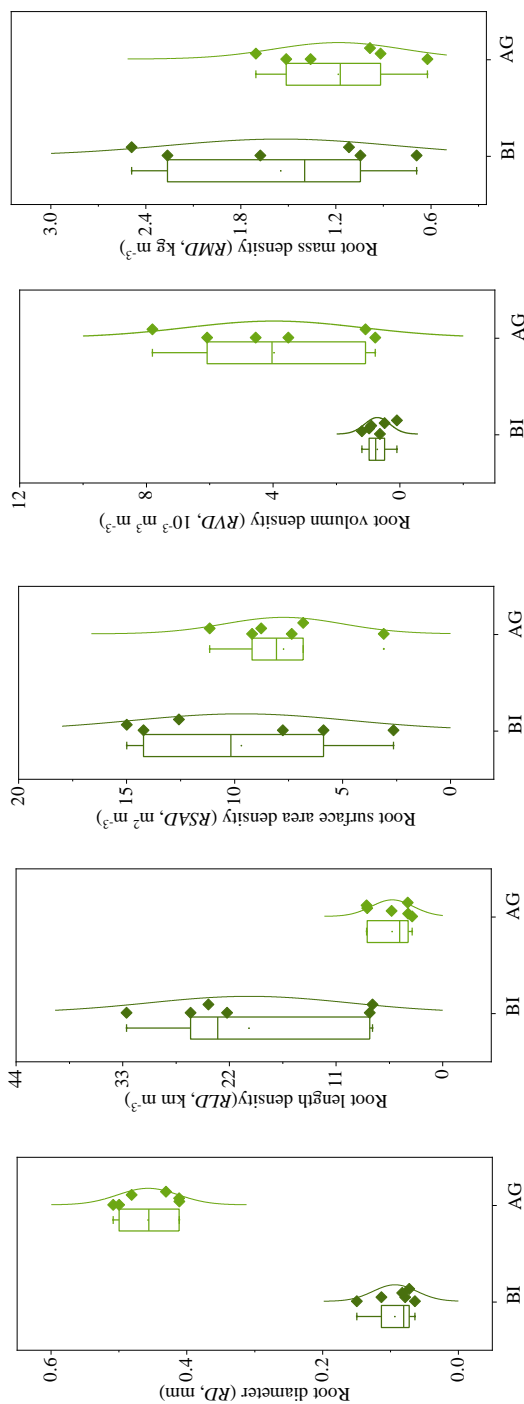


Figure 1 Root traits of RD, RLD, RSAD, RVR and RMD between *Boihriochloa ischecum* (Linn.). Keng and *Artemisia vestita* Wall. ex Bess herbaceous plants

648
 649
 650
 651

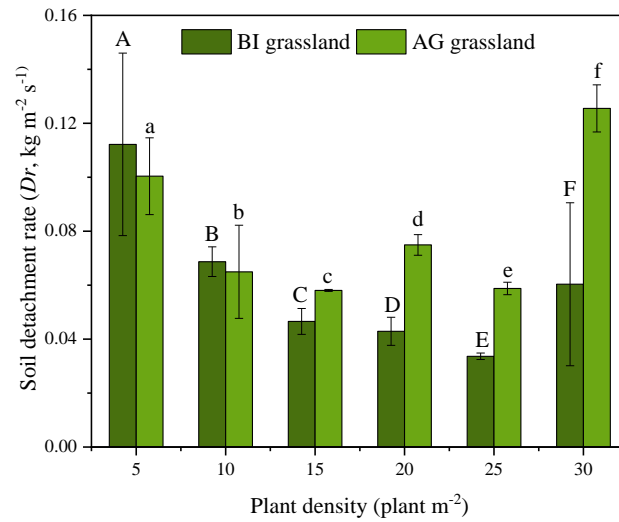


Figure 2 Soil detachment rate (D_r) in different plant densities.

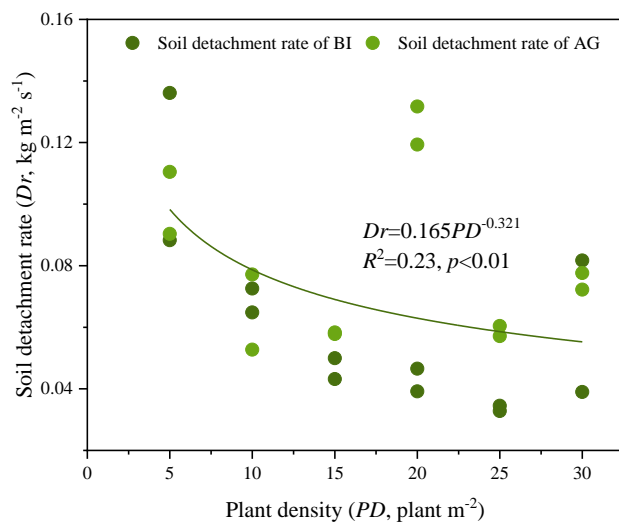


Figure 3 Soil detachment rate (Dr) as a power function of plant density (PD)

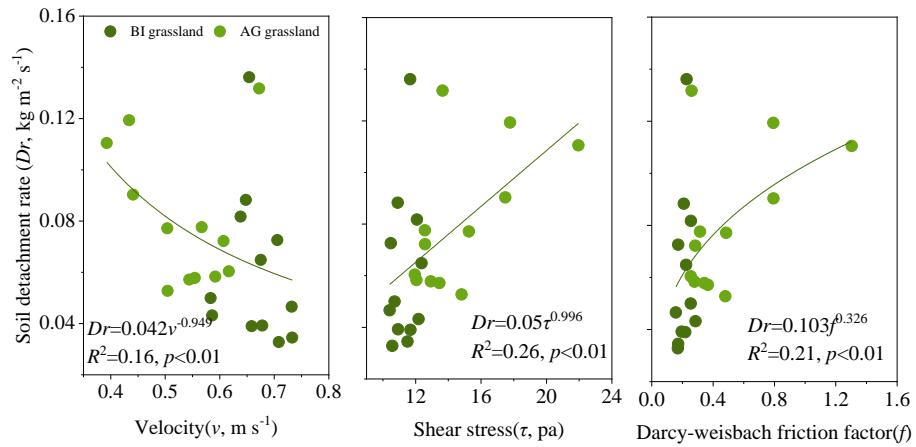


Figure 4 Soil detachment rate (Dr) as a power function of velocity (v), shear stress (τ) and darcy-weisbach friction factor(f)

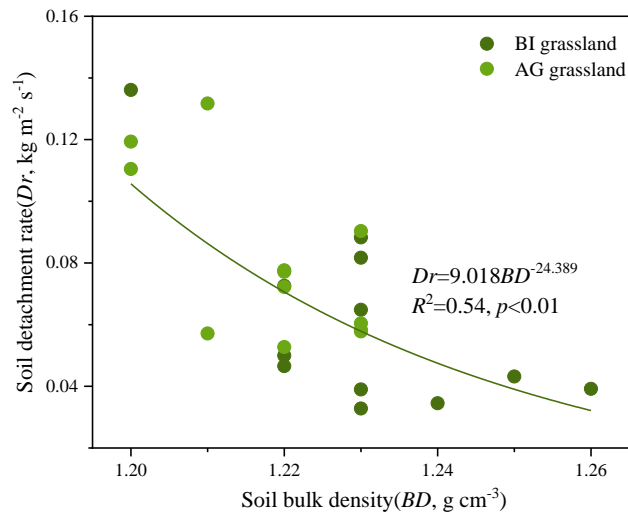


Figure 5 Soil detachment rate (Dr) as power function of soil bulk density (BD)

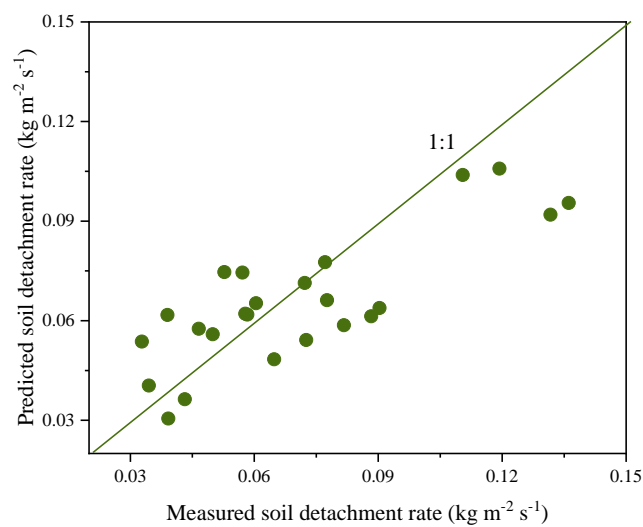


Figure 7 Compared with measured soil detachment rate and soil detachment rate



Table 1 Variation of soil properties by plant growth between *Bothriochloa ischcemum* (Linn.) Keng (BI) grasslands and *Artemisia vestita* Wall. ex Bess (AG) grasslands

| Plant density plant m ⁻² | Bulk density (g cm ⁻³) | | Cohesion (KPa) | | Water stable aggregate (%) | | Soil organic matter (g kg ⁻¹) | | Soil erodibility | |
|--|---------------------------------------|------|-------------------|------|-------------------------------|------|--|------|------------------|------|
| | BI | AG | BI | AG | BI | AG | BI | AG | BI | AG |
| 5 | 1.22 | 1.22 | 4.18 | 4.36 | 1.6 | 0.63 | 6.6 | 4 | 0.39 | 0.4 |
| 10 | 1.23 | 1.22 | 4.83 | 4.49 | 1.91 | 1.19 | 7.22 | 5.09 | 0.39 | 0.39 |
| 15 | 1.24 | 1.23 | 4.95 | 4.58 | 2.05 | 0.97 | 7.69 | 5.97 | 0.38 | 0.39 |
| 20 | 1.24 | 1.22 | 4.68 | 4.68 | 2.23 | 0.9 | 12.75 | 8.11 | 0.34 | 0.38 |
| 25 | 1.24 | 1.22 | 4.72 | 4.54 | 2.06 | 0.48 | 13.15 | 6.35 | 0.34 | 0.39 |
| 30 | 1.23 | 1.21 | 4.1 | 4.68 | 1.95 | 0.09 | 16.75 | 7.64 | 0.31 | 0.38 |
| Bare control | 1.27 | | 4.3 | | 2.88 | | 3.31 | | 0.4 | |



Table 2 Correlation coefficient among of soil properties, root traits and soil detachment rate

| | v | τ | f | Coh | BD | SWAC | SOC | K | RD | RMD | RLD | RSAD | RVD |
|------|----------|----------|----------|---------|----------|--------|--------|--------|----------|---------|----------|--------|-------|
| RD | -0.717** | 0.656** | 0.697** | 0.014 | -0.312 | -0.114 | -0.626 | 0.192 | 1 | | | | |
| RMD | 0.377 | -0.564** | -0.472* | 0.617** | 0.379 | 0.261 | 0.000 | -0.296 | -0.148 | 1 | | | |
| RLD | 0.700** | -0.718** | -0.721** | 0.440* | 0.423* | 0.274 | 0.467 | -0.263 | -0.685** | 0.654** | 1 | | |
| RSAD | 0.390 | -0.478 | -0.446* | 0.624* | 0.351 | 0.005 | -0.034 | -0.295 | -0.037 | 0.872** | 0.562** | 1 | |
| RVD | -0.246 | 0.116 | 0.179 | 0.318 | -0.157 | 0.012 | -0.550 | -0.050 | 0.673** | 0.412* | -0.189 | 0.510* | 1 |
| Dr | -0.441* | 0.535** | 0.503* | -0.244 | -0.700** | -0.213 | -0.443 | 0.190 | 0.280 | -0.361 | -0.560** | -0.351 | 0.104 |

Note: * $p < 0.05$, ** $p < 0.01$, $n = 24$

Where v, τ and f are velocity, shear stress and Darcy-weisbach friction factor of overland flow. Coh, BD, SWAC, SOC and K are soil properties of cohesion, bulk density, water stable aggregate, organic matter and soil erodibility. RD, RMD, RLD, RSAD and RVD are root traits of root diameter, root mass density, root length density, root surface area density and root volume density.



Table 3 Variation of velocity, shear stress, Darcy-weisbach friction factor between *Bothriochloa ischaemum* (Linn.). Keng (BI) grasslands and *Artemisia vestita* Wall. ex. Bess (AG) grasslands

| Plant density plant m ⁻² | Velocity m s ⁻¹ | | shear stress Pa | | Darcy-weisbach friction factor | |
|--|-------------------------------|-------------|--------------------|--------------|--------------------------------|-------------|
| | BI | AG | BI | AG | BI | AG |
| 5 | 0.651±0.004 | 0.417±0.034 | 11.289±0.541 | 19.724±3.159 | 0.219±0.013 | 1.049±0.361 |
| 10 | 0.690±0.021 | 0.504±0.000 | 11.424±1.329 | 15.038±0.310 | 0.198±0.036 | 0.482±0.004 |
| 15 | 0.585±0.002 | 0.573±0.027 | 11.451±1.038 | 12.476±0.623 | 0.270±0.022 | 0.311±0.045 |
| 20 | 0.705±0.038 | 0.587±0.028 | 10.676±0.368 | 12.576±0.008 | 0.177±0.027 | 0.299±0.022 |
| 25 | 0.721±0.017 | 0.581±0.051 | 11.045±0.661 | 12.705±1.068 | 0.172±0.001 | 0.311±0.079 |
| 30 | 0.684±0.014 | 0.553±0.169 | 11.892±0.278 | 15.716±2.914 | 0.237±0.027 | 0.527±0.377 |